minerals

MDPI

Article

Response Surface Methodology-Based Evaluation of Chemical and Biological Leaching Performance of a Complex Sphalerite Ore

Zehra Çetinkaya [1], Seda Demirci [2,*], Ercüment Koç [3] and Durmuş Çetinkaya [2]

[1] Central Research Laboratory, Cukurova University, Adana 01330, Türkiye; zaltincelep@cu.edu.tr
[2] Aladağ Vocational School, Cukurova University, Adana 01330, Türkiye; dcetinkaya@cu.edu.tr
[3] Metallurgy and Materials Engineering Department, Atatürk University, Erzurum 25010, Türkiye; ercument.koc@atauni.edu.tr
* Correspondence: demircis@cu.edu.tr

Abstract

In this study, the chemical leaching and bioleaching behaviors of a complex carbonate-rich sphalerite ore were statistically evaluated using Response Surface Methodology (RSM) based on Central Composite Design (CCD) and the effects of process parameters on Zn and Fe recovery were assessed. The maximum Zn recovery obtained in the chemical leaching process was 59.16%, while the maximum Zn recovery in the biological leaching process was determined to be 37.26%. Statistical analyses showed that the solid-to-liquid ratio and leaching time had a significant effect on chemical leaching performance, while the effect of Fe(II) concentration on biological leaching performance was limited. During biological leaching, pH increases occurred due to the ore's carbonate-rich structure, and periodic sulfuric acid adjustments were made to maintain suitable biological leaching conditions. The findings indicate that carbonate-rich mineral structures significantly influence both chemical and biological leaching behavior, and that this effect must be taken into account in the processing of complex sphalerite ores.

Keywords: sphalerite; bioleaching; chemical leaching; *Acidithiobacillus ferrooxidans*; response surface methodology (RSM)

1. Introduction

Sphalerite is the most important zinc ore worldwide. Zinc finds applications in many sectors, including the steel, metallurgy, machinery, electrical, and chemical industries [1,2]. Lead, carbonate, and iron minerals may be found as associated minerals alongside sphalerite ores [3,4]. Carbonate minerals are common gangue components in many complex sulfide ores and can significantly influence metal extraction processes. In hydrometallurgical operations, their dissolution consumes acid and alters solution chemistry, whereas in pyrometallurgical processing they may increase energy demand, contribute to slag formation and gas emissions [5–7].

Among hydrometallurgical methods for zinc recovery from sphalerite, chemical leaching and bioleaching are widely employed. Reagents with oxidizing properties are generally used, and in chemical leaching, elevated temperatures and higher acid concentrations enhance dissolution rates and metal recovery [3]. The mechanism of chemical leaching can be mainly attributed to acid-promoted dissolution under acidic conditions [8]. However,

Check for updates

Academic Editor: Dianwen Liu

Received: 18 May 2026
Revised: 13 June 2026
Accepted: 18 June 2026
Published: 29 June 2026

Copyright: © 2026 by the authors. Licensee MDPI, Basel, Switzerland. This article is an open access article distributed under the terms and conditions of the Creative Commons Attribution (CC BY) license.

high reagent consumption, the formation of passivation layers such as elemental sulfur on the mineral surface, and environmental impacts are notable drawbacks.

Bioleaching is an environmentally advantageous technique that facilitates the oxidation of sulfide minerals by microorganisms such as *Acidithiobacillus ferrooxidans* (*A. ferrooxidans*) [9–11]. The Fe^{2+}/Fe^{3+} redox cycle is critical to bioleaching, as the resulting Fe^{3+} oxidizes sulfide minerals such as sphalerite, thereby facilitating their dissolution [3,12–14]. Bioleaching efficiency depends on physicochemical parameters such as pH, iron concentration, and solid-to-liquid ratio [15–19]. Studies in the literature on sphalerite leaching indicate that dissolution efficiency is influenced by parameters such as acid concentration, temperature, solid-to-liquid ratio, and reaction time [3].

Carbonate-rich minerals can increase acid consumption by raising the pH of the system, which may lead to jarosite precipitation. Jarosite slows down zinc extraction by coating the mineral surface [2,20]. Additionally, the elemental sulfur layer formed on the sphalerite surface as a reaction product can cause passivation by preventing reagents from accessing the mineral surface [20]. High solid-to-liquid ratios may create mass transfer limitations and reduce reagent accessibility to mineral surfaces [21]. Furthermore, limited oxygen transfer and the inability to precisely control operating parameters are other key technical constraints that reduce bioleaching efficiency [22].

Although extensive research on sphalerite leaching exists in the literature, studies comparing chemical and biological methods for the processing of complex ores with high carbonate content under realistic industrial conditions remain limited. In particular, the combined effects of high solid-to-liquid ratio and the buffering behavior of carbonate-rich media in bioreactor systems need to be investigated in detail for the development of efficient industrial processes.

In this study, the effects of process parameters on chemical leaching with sulfuric acid and biological leaching methods using *A. ferrooxidans* for zinc recovery from complex sphalerite ore obtained from the Kozan-Horzum (Adana) region were investigated using Response Surface Methodology (RSM) based on Central Composite Design (CCD). Additionally, the study aimed to identify the fundamental mechanisms controlling dissolution in both systems and to determine the primary factors influencing zinc recovery. The findings contribute to the development of more efficient and environmentally friendly processes for the processing of complex zinc ores. The novelty of this study lies in the statistically optimized analysis of variables in chemical leaching and bioreactor-based biological leaching methods of carbonate-rich complex sphalerite ore, focusing particularly on parameter interactions, process behavior, and zinc dissolution performance. It should be noted that, since the two processes inherently require different independent variables, the comparison presented in this study is not based on identical experimental conditions, but rather on the performance, dominant process parameters, and operating characteristics of each system evaluated under its own optimum conditions. The solid-to-liquid ratio, which was investigated in both systems, served as the primary basis for a mechanistic comparison between the two processes.

2. Materials and Methods

2.1. Preparation of Sphalerite Sample

The sphalerite ore used in this study was obtained from a lead-zinc mine located in the Kozan region of Adana, Türkiye. The run-of-mine material was first crushed to below 1 mm using a laboratory-scale jaw crusher (Ünal Engineering, Izmir, Türkiye). Subsequently, the crushed material was homogenized, and representative subsamples were prepared using the cone and quartering method under laboratory conditions. For the grinding process, 500 g of ore was ground in a laboratory ball mill (Jeotest, Ankara, Türkiye) using 2000 g

of steel balls of various sizes until the particle size was reduced to below 75 μm. The resulting slurry was wet screened through a 75 μm sieve, and the undersize fraction was subsequently dried in an oven at 105 °C (Figure 1).

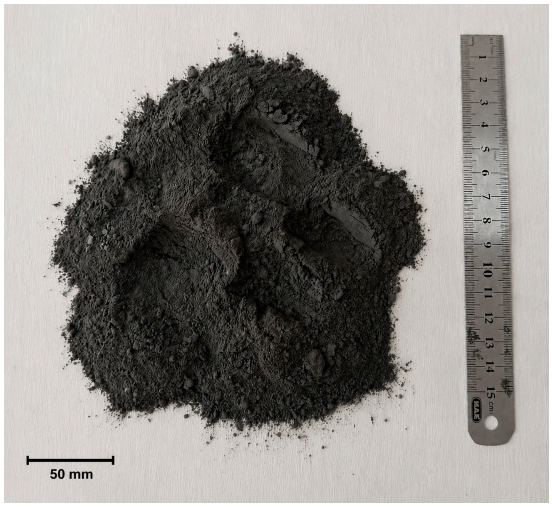


Figure 1. Sphalerite ore sample ground to below 75 μm in a laboratory ball mill.

2.2. Microorganisms and Culture Medium

The bacterium *A. ferrooxidans* (DSM 583), obtained from the Deutsche Sammlung von Mikroorganismen und Zellkulturen, was used in the biological leaching experiments, and a 9K medium was used for bacterial growth. The 9K medium consisted of the following analytical-grade components: 0.4 g/L $(NH_4)_2SO_4$, 0.4 g/L $MgSO_4 \cdot 7H_2O$, 0.2 g/L KH_2PO_4, 0.1 g/L KCl, and 55.6 g/L $FeSO_4 \cdot 7H_2O$. During the pre-cultivation stage, the pH of the culture medium was adjusted to 1.8–2.0 using sulfuric acid to support bacterial growth. The prepared medium was sterilized in an autoclave (Nüve, Ankara, Türkiye) at 121 °C for 15 min. The inoculum used in the bioleaching experiments was obtained from actively growing cultures, and the initial bacterial concentration was approximately 10^8 cells/mL. After the pre-cultivation stage, Fe(II) was added at different concentrations to the iron-free medium prepared in the bioreactor as a variable parameter in the bioleaching experiments.

2.3. Chemical Leaching Experiments

Chemical leaching experiments were performed using sphalerite samples with a particle size of −75 μm in a three-neck glass reactor (ISOLAB, Eschau, Germany) with a working volume of 250 mL. To prevent evaporation during the experiments, the system was equipped with a reflux condenser, and the leaching tests were conducted with a suspension volume of 100 mL. The experimental setup for sulfuric acid leaching is presented in Figure 2a. Throughout all experiments, the agitation speed was maintained at 800 rpm. At the end of the experiments, the slurry was filtered for solid–liquid separation. The concentrations of dissolved Zn and Fe in the filtrate were determined using an atomic absorption spectrometer (AAS). The solid residues were dried in an oven at 105 °C, followed by mineralogical analyses.



(**a**) (**b**)

Figure 2. Experimental setups for chemical leaching (**a**) and bioleaching (**b**).

2.4. Bioleaching Experiment

Bioleaching experiments were performed in a 16-litre plexiglass bioreactor equipped with a mechanical stirrer (Mtops, Seoul, Republic of Korea) (Figure 2b). The working volume was kept constant at 16 L. For each experiment, approximately 10% (*v*/*v*) of the working volume, 1600 mL of active growth-phase *A. ferrooxidans* bacterial culture, was inoculated. The remaining volume was supplemented with iron-free 9K medium. Fe(II) was added to the system in amounts appropriate to the experimental design. Aeration was performed in the bioreactor to ensure oxygen transfer and maintain microbial activity. Aeration was provided through a filtered system using a dual-outlet air pump with a nominal capacity of 7 L/min (approximately 0.44 vvm). Continuous aeration and mechanical stirring at 150 rpm were applied throughout the experiment to ensure homogeneous mixing.

Bioleaching was conducted under controlled conditions at a temperature of 30 ± 2 °C for 20 days. During the experiments, pH was monitored every other day using a WTW S-720 pH meter. Due to the carbonate-rich nature of the ore, acid consumption and pH increases occurred during the bioleaching process. Therefore, to maintain the pH at the design-specified initial value and to prevent sudden pH fluctuations that could negatively affect bacterial activity, pH was periodically adjusted using 18 M sulfuric acid. During the bioleaching process, 2 mL samples were collected every three days and filtered through 0.2 µm membrane filters for solid–liquid separation. The total volume of sulfuric acid added during the experiment was not systematically recorded; therefore, the total acid consumption could not be quantitatively calculated. The concentrations of dissolved Zn and Fe in the collected liquid samples were determined using atomic absorption spectroscopy (AAS). The filtered solid fractions were dried in an oven at 105 °C, and mineralogical analyses were performed.

In biological leaching experiments, Fe(II) was added externally as an independent variable at specified concentrations. Since the Fe concentration measured in the solution could originate from both the ore and the added Fe(II), Fe recovery was calculated based on the total Fe content of the ore determined by XRF and AAS analyses. At the end of each experiment, the Fe concentration measured in the leaching solution was used to calculate the percentage of Fe dissolved from the ore after deducting the contribution of the initially

added Fe(II). This distinction was considered important for the accurate interpretation of Fe recovery in relation to sphalerite dissolution.

2.5. Experiment Design

In this study, the effects of process variables and their interactions on the response were investigated using Response Surface Methodology (RSM) based on a Central Composite Design (CCD), implemented in Design-Expert 13 software (Stat-Ease Inc., Minneapolis, MN, USA). Within the RSM-CCD space, factorial, axial, and center points were employed to ensure reliable estimation of the model variance [23,24]. According to the design matrix, factor levels were coded as −1, 0, and +1. In the chemical leaching experiments conducted with sulfuric acid, solid-to-liquid ratio, leaching time, temperature, and acid concentration were selected as independent variables. For the bioleaching experiments conducted in the bioreactor, pH, solid-to-liquid ratio, and Fe(II) concentration were selected as independent variables. In all experiments, the effects of these variables on the recovery efficiencies of Zn and Fe were statistically analyzed. The experimental conditions are summarized in Tables 1 and 2.

Table 1. Chemical leaching parameters.

Parameters	Code	−a	−1	0	+1	+a
Temperature (°C)	A	20	40	60	80	100
S/L (% *w*/*v*)	B	1	3	6	9	12
Time (min)	C	30	45	60	75	90
Acid Concentration (M)	D	1	2	3	4	5

Table 2. Bioleaching operating conditions.

Parameters	Code	−a	−1	0	+1	+a
pH	A	1.2	1.4	1.6	1.8	2
S/L (% *w*/*v*)	B	1	3	6	9	12
Fe(II) (g/L)	C	0	2	4	6	8

The response variables were modeled using a multivariate polynomial regression equation including linear and quadratic terms. The second-order regression model developed for the estimation of the response variables is presented in Equation (1). In this equation, X*i* and Xj are the coded values of the independent variables, Y represents the predicted response; b_0 is the intercept term; b_i, b_{ii}, and b_{ij} represent the linear, quadratic, and interaction coefficients, respectively; and k is the number of factors, and ε is the random error term [25]. The significance and adequacy of the developed models were evaluated using analysis of variance (ANOVA), adjusted R^2, and predicted R^2 values. The effects of the process parameters on metal recovery were interpreted using regression coefficients, contour plots, and response surface plots.

$$Y = b_0 + \sum_{i=1}^{k} b_i X_i + \sum_{i=1}^{k} b_{ii} X_i^2 + \sum_{i=1}^{k-1} \sum_{J=i+1}^{k} b_{ij} X_i X_j + \varepsilon \quad (1)$$

3. Results

3.1. Chemical Characterization of the Sphalerite Ore

The chemical composition of the sample was determined using X-ray fluorescence (XRF) analysis using a Minipal 4 (PANalytical, B. V., Almelo, The Netherlands). The concentrations of Zn and Fe in the solution samples were measured using an atomic absorption spectrometer (AAS) (PerkinElmer Inc., Waltham, MA, USA). Mineralogical

analyses were performed using a Rigaku Miniflex II diffractometer (Rigaku Corporation, Tokyo, Japan) with Cu Kα radiation (λ = 1.5406 Å) operated at 40 kV and 30 mA, with a step size of 0.02° over a 2θ range of 5–90°. The surface morphology and elemental distribution of the sphalerite sample were examined using SEM-EDX analysis with an FEI Quanta 650 Field Emission Scanning Electron Microscope (FE-SEM) (FEI Company, Hillsboro, OR, USA) before and after leaching.

Sphalerite samples ground to less than 75 microns were pelleted for XRF analysis using Merck brand Hoechst wax C micropowder (Merck KGaA, Darmstadt, Germany). The chemical composition of the sphalerite ore was determined by X-ray fluorescence (XRF) analysis. The results showed that the sample mainly consisted of CaO (41.65%), ZnO (19.51%), Al_2O_3 (0.95%), SiO_2 (0.56%), SO_3 (13.26%), Fe_2O_3 (4.62%), PbO (2.40%), BaO (9.67%), Loss on Ignition (LOI) (6.60%), and other minor components (0.78%). The high CaO content confirms the carbonate-rich nature of the ore and suggests significant acid consumption due to carbonate dissolution during leaching processes. Furthermore, elemental analysis of the ore sample by atomic absorption spectroscopy (AAS) revealed Zn and Fe contents of 14.87% and 3.32%, respectively. These results are consistent with the XRF findings and support the presence of a complex carbonate-rich sulfide ore structure.

3.2. Mineralogical and Morphological Analysis

X-ray Diffraction (XRD) analysis revealed the presence of sphalerite (ZnS), galena (PbS), barite ($BaSO_4$), pyrite (FeS_2), and calcite ($CaCO_3$) mineral phases in the ore sample, confirming the complex mineralogical structure and high carbonate content of the ore (Figure 3). The coexistence of sulfide and carbonate minerals is expected to influence the leaching behavior through both metal dissolution and acid-consuming reactions. SEM–EDS analysis of the feed sample (Figure 4) showed irregular crystal structures, microcracks, and porous surface morphologies, which may increase reagent–mineral contact and facilitate the dissolution of zinc-bearing minerals during leaching. The Au peaks observed in the SEM–EDS spectra originated from the gold coating applied prior to analysis to improve surface conductivity.

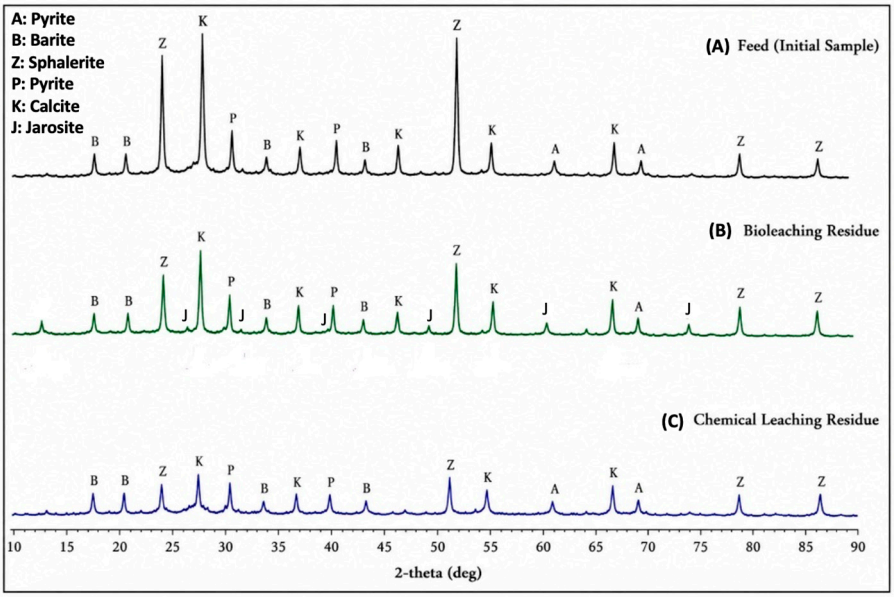


Figure 3. XRD patterns of (**A**) the feed (initial sample), (**B**) the bioleaching residue, and (**C**) the chemical leaching residue.

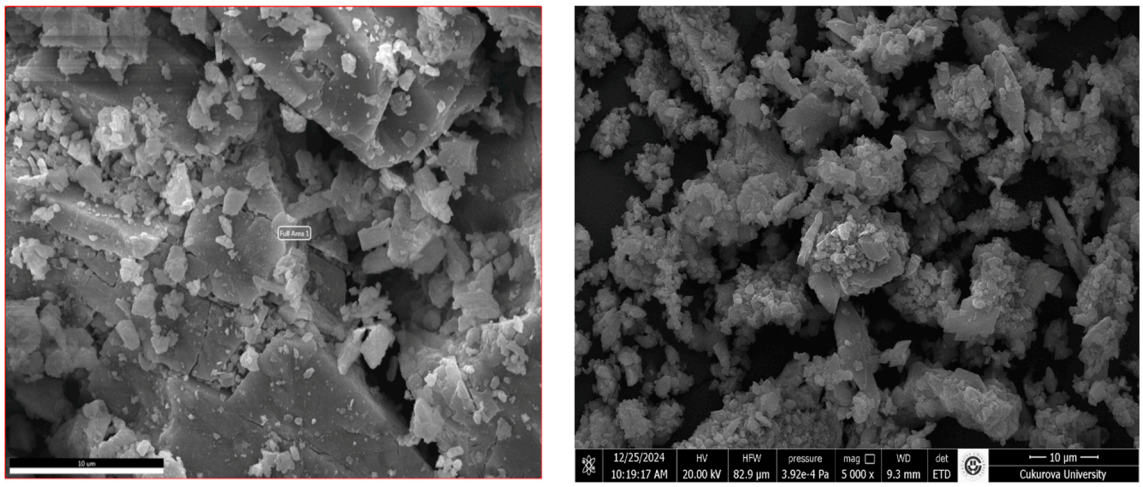


Figure 4. (**a**) SEM micrograph of the sphalerite sample illustrating surface morphology, particle distribution, and mineralogical associations prior to leaching. EDX analysis was performed over the entire scanned area (full area). The elemental composition obtained from EDX analysis was C: 3.10%, O: 24.78%, Zn: 2.71%, S: 3.05%, Ca: 59.23%, Ba: 3.97%, and Au: 3.17%. (**b**) SEM micrograph of the sphalerite residue illustrating surface morphology and mineralogical associations after bioleaching. EDX analysis was performed over the entire scanned area (full area). The elemental composition obtained from EDX analysis was C: 15.77%, O: 39.79%, Mg: 0.59%, S: 3.23%, Ca: 25.60%, Ba: 1.59%, Fe: 1.79%, Zn: 3.10%, Au: 8.54%.

XRD and SEM–EDS analyses of the leaching residues provided complementary information regarding the mineralogical and surface changes occurring during the leaching processes. In the chemical leaching residue, the intensity of sphalerite peaks decreased markedly compared with the feed sample, indicating partial dissolution of zinc-bearing minerals and supporting the higher Zn recovery obtained in chemical leaching experiments. In the bioleaching residue, the persistence of sphalerite peaks suggests that zinc-containing sulfide minerals were only partially dissolved. Additionally, weak diffraction peaks observed in the bioleaching residue may indicate the formation of secondary iron-containing sulfate phases during the bioleaching process. SEM–EDS results further support these observations. Compared with the feed sample, the reduced Ca content in the bioleaching residue suggests dissolution of carbonate minerals, while the increased oxygen content is consistent with the formation of oxidation products and secondary surface phases. Overall, the mineralogical and surface characterization results indicate that chemical leaching promoted more extensive zinc dissolution than bioleaching under the conditions investigated.

3.3. Statistical Modeling and Model Validation for Chemical Leaching

The experimental design for sulfuric acid leaching was analyzed based on a central composite design. The effects of solid-to-liquid ratio, acid concentration, leaching time, and temperature were evaluated. Table 3 presents the experimental conditions used in the 27 runs and the corresponding responses (Zn and Fe recovery rates). As shown in Table 3, the leaching recovery rate for Zn ranged from 12.36% to 59.16%, while the Fe recovery rate ranged from 34.16% to 50.03%. The results indicate that the solid-to-liquid ratio significantly influenced metal recovery. At high solid-to-liquid ratios, Zn recovery decreased considerably, suggesting that high pulp density negatively affected the leaching efficiency. The increase in Fe recovery with increasing solid-to-liquid ratio may be associated with the simultaneous dissolution of multiple iron-bearing mineral phases in the ore. Pyrite (FeS_2), identified by XRD analysis, is one of the iron-bearing mineral phases whose dissolution may contribute to the increased Fe recovery observed at

high solid-to-liquid ratios. Zn recovery depends on reactive contact with the ZnS surface. Therefore, it is negatively affected at high pulp densities. This result indicates that pulp density exerts opposing effects on Fe and Zn recovery [2,3].

Table 3. Experimental design matrix and corresponding Zn and Fe recoveries for chemical leaching.

Run	Temperature (A) (°C)	S/L (% *w*/*v*) (B) (%)	Time (C) (min.)	Acid Concentration (D) (M)	Zn (%)	Fe (%)
1	20	6	60	3	46.87	43.91
2	40	9	45	2	36.35	45.21
3	100	6	60	3	45.56	44.17
4	40	9	75	2	18.97	46.45
5	80	9	75	2	33.05	47.35
6	40	3	45	2	22.94	34.56
7	40	3	75	4	59.16	43.67
8	80	3	45	2	23.01	38.64
9	80	9	45	2	49.65	44.43
10	40	3	75	2	30.98	39.87
11	60	6	90	3	31.56	46.87
12	80	3	45	4	21.95	40.11
13	40	9	75	4	24.89	50.03
14	60	6	60	3	55.36	44.11
15	80	9	45	4	19.29	47.64
16	40	3	45	4	34.44	42.31
17	80	9	75	4	18.24	48.36
18	60	12	60	3	12.36	48.59
19	60	1	60	3	24.87	34.16
20	60	6	60	3	57.63	45.93
21	60	6	60	1	30.19	37.94
22	40	9	45	4	28.01	48.91
23	60	6	30	3	29.67	44.17
24	80	3	75	4	45.26	44.65
25	60	6	60	3	56.96	45.37
26	60	6	60	5	28.57	49.54
27	80	3	75	2	34.24	39.34

The regression models are presented in Equations (2) and (3). In the ANOVA analysis, the independent variables were coded as temperature (A), solid-to-liquid ratio (B), time (C), and acid concentration (D). A second-order regression model was applied for both Zn and Fe leaching. The obtained R^2 values were 0.9938 for Zn leaching and 0.9631 for Fe leaching. The predicted R^2 values were 0.9661 for Zn and 0.80 for Fe, while the adjusted R^2 values were 0.9865 and 0.92, respectively. The close agreement between these values indicates that the developed models have good predictive capability. The final regression equations were constructed using statistically significant coefficients. The statistically significant quadratic terms A^2, B^2, C^2, D^2 indicate that the relationship between process variables and Zn recovery is not linear. The parameters reduce Zn recovery both below and above the ranges examined.

$$\text{Zn (\%)} = +56.65 - 0.5696A - 2.86B + 1.37C - 0.0496D + 2.19AB + 0.2894AC - 4.53AD - 6.59BC - 6.08BD + 3.66CD - 2.60A^2 - 9.50B^2 - 6.50C^2 - 6.81D^2 \quad (2)$$

$$\text{Fe (\%)} = +45.14 + 0.0013A + 3.50\,B + 0.9713C + 2.21D - 0.3219AB - 0.0094AC - 0.3694BC - 0.4269BD - 0.1519CD - 0.2447A^2 - 0.9109B^2 + 0.1253C^2 - 0.3197D^2 \quad (3)$$

According to the ANOVA results (Tables 4 and 5), the solid-to-liquid ratio and leaching time had significant individual effects on Zn recovery, while Fe recovery was mainly influenced by the solid-to-liquid ratio, leaching time, and acid concentration. The obtained models and parameters were found to be statistically significant at the $p < 0.05$ level. According to the RSM analysis, the lack-of-fit F values calculated for Zn (1.94) and Fe (1.86) were insignificant, indicating that model misfit was not a significant issue and that the developed models adequately represented the experimental data. The parameter interactions affecting Zn recovery were identified as temperature with solid-to-liquid ratio (AB), temperature with acid concentration (AD), solid-to-liquid ratio with leaching time (BC), solid-to-liquid ratio with acid concentration (BD), and leaching time with acid concentration (CD) (Table 4). For Fe recovery, the B^2 term was identified as particularly significant (Table 5).

Table 4. Analysis of variance table for Zn recovery.

Source	Sum of Squares	df	Mean Square	F-Value	*p*-Value	
Model	4650.46	14	332.18	136.67	<0.0001	significant
A-Temperature (°C)	7.79	1	7.79	3.20	0.0987	
B-S/L (% *w*/*v*)	195.80	1	195.80	80.56	<0.0001	
C-Time (min.)	45.18	1	45.18	18.59	0.0010	
D-Acid Concentration (M)	0.0590	1	0.0590	0.0243	0.8788	
AB	76.87	1	76.87	31.63	0.0001	
AC	1.34	1	1.34	0.5513	0.4721	
AD	328.24	1	328.24	135.06	<0.0001	
BC	694.98	1	694.98	285.95	<0.0001	
BD	590.85	1	590.85	243.11	<0.0001	
CD	214.40	1	214.40	88.22	<0.0001	
A^2	143.88	1	143.88	59.20	<0.0001	
B^2	1924.11	1	1924.11	791.68	<0.0001	
C^2	900.50	1	900.50	370.51	<0.0001	
D^2	988.12	1	988.12	406.56	<0.0001	
Residual	29.17	12	2.43			
Lack of Fit	26.44	10	2.64	1.94	0.3871	not significant
Pure Error	2.72	2	1.36			
Cor Total	4679.63	26				

Table 5. Analysis of variance table for Fe recovery.

Source	Sum of Squares	df	Mean Square	F-Value	*p*-Value	
Model	467.93	14	33.42	22.37	<0.0001	significant
A-Temperature (°C)	0.0000	1	0.0000	0.0000	0.9961	
B- S/L (% *w*/*v*)	294.63	1	294.63	197.20	<0.0001	
C-Time (min.)	22.64	1	22.64	15.15	0.0021	
D-Acid Concentration (M)	117.17	1	117.17	78.42	<0.0001	
AB	1.66	1	1.66	1.11	0.3129	
AC	0.0014	1	0.0014	0.0009	0.9760	
AD	3.83	1	3.83	2.56	0.1353	
BC	2.18	1	2.18	1.46	0.2500	
BD	2.92	1	2.92	1.95	0.1877	
CD	0.3691	1	0.3691	0.2470	0.6282	
A^2	1.28	1	1.28	0.8549	0.3734	

Table 5. *Cont.*

Source	Sum of Squares	df	Mean Square	F-Value	*p*-Value	
B^2	17.70	1	17.70	11.85	0.0049	
C^2	0.3350	1	0.3350	0.2242	0.6443	
D^2	2.18	1	2.18	1.46	0.2503	
Residual	17.93	12	1.49			
Lack of Fit	16.19	10	1.62	1.86	0.3994	not significant
Pure Error	1.74	2	0.8689			
Cor Total	485.85	26				

Temperature (A) had no statistically significant effect on Zn recovery during leaching of sphalerite ore with sulfuric acid, according to ANOVA results ($p = 0.0987$). Although temperature was not statistically significant as an individual factor, its interaction with solid-to-liquid ratio and acid concentration significantly influenced Zn recovery. This indicates that the effect of temperature on Zn recovery is not independent but a variable conditioned by other process variables. Although the temperature variable alone is not statistically significant, it can become significant at different combinations of solid-to-liquid ratio and acid concentration. This result indicates that the influence of temperature depends on its interaction with other process variables. At low solid-to-liquid ratios, increasing temperature enhances reagent–mineral interactions and promotes Zn dissolution. Conversely, at high solid-to-liquid ratios, the increased pulp density restricts reactant access to the mineral surface, thereby suppressing the effect of temperature on Zn dissolution [3,20]. Similarly, at moderate acid concentrations, temperature accelerates Zn dissolution, while at low or high acid concentrations, the carbonate buffering effect limits the contribution of temperature to Zn dissolution [3,26].

To evaluate the suitability of the developed regression models for Zn and Fe recovery, basic diagnostic plots were analyzed. As shown in Figure 5a, the fact that most of the data points in the regression model align along the diagonal indicates a strong fit between the predicted values and the experimental data. This demonstrates that the model has predictive capability within its confidence intervals. Furthermore, the absence of any significant deviation in the data points demonstrates that the model effectively represents the relationship between the process variables under investigation and the response variable within the operating range. Figure 5b shows the relationship between residuals and the experimental sequence. The lack of systematic variation in the data points indicates that there is no time-dependent effect. This is important for identifying the effects of possible device deviations, changes in environmental conditions, or personal errors that may have occurred during the experiments. The dispersion of the data around the zero line indicates that the experiments are independent and that there are no systematic errors in the experiments. Figure 5c shows the distribution of the residuals. The random distribution of the data points around the zero line indicates that the variance is constant and that the estimates do not exhibit any systematic bias. Figure 5d shows a linear distribution of residuals in the normal probability plot. The absence of skewness in the plots indicates that the responses fit the model and that the prediction errors in the model are randomly distributed.

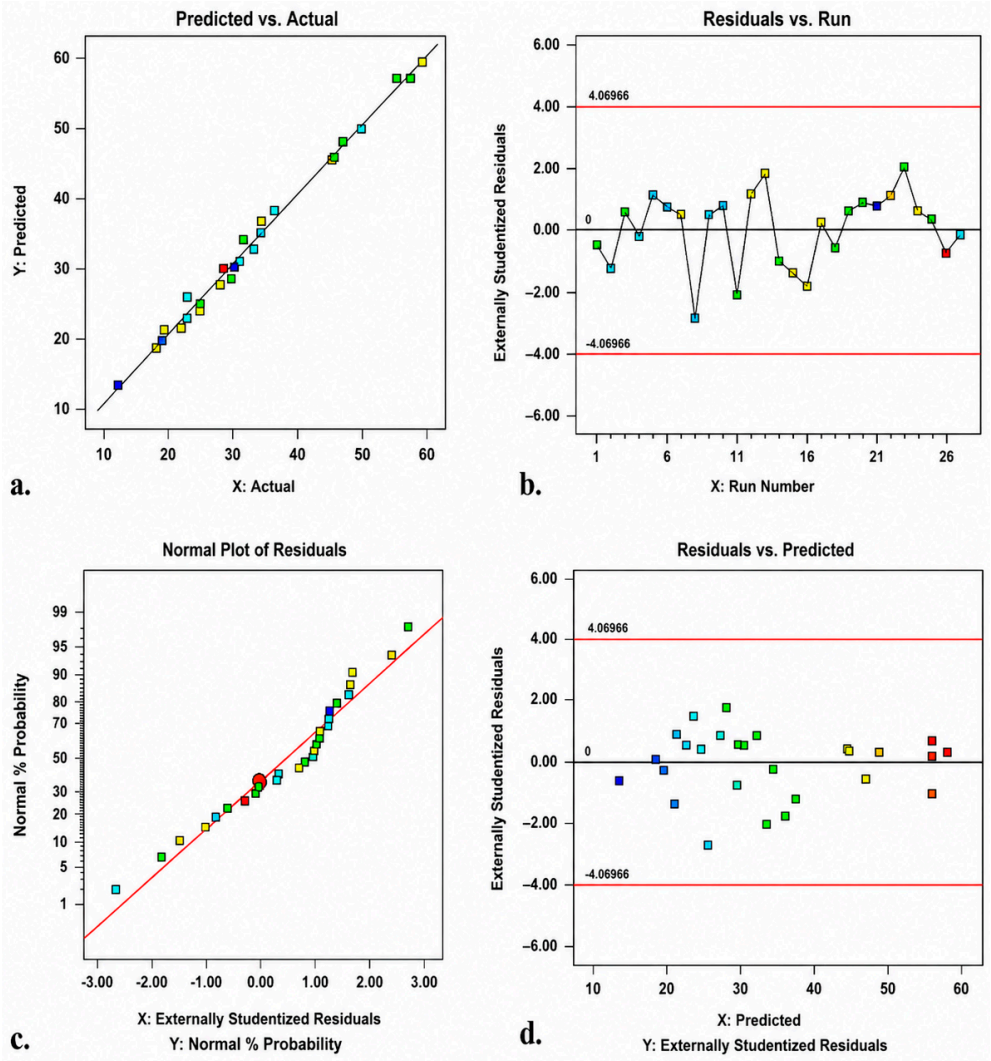


Figure 5. Diagnostic plots for Zn recovery: (**a**) predicted values vs. actual values, (**b**) internally studentized residuals vs. run number, (**c**) normal probability plot of internally studentized residuals, and (**d**) internally studentized residuals vs. predicted values.

The parameter interactions obtained, which significantly influenced the responses, were used to plot the three-dimensional (3D) graphs shown in Figure 6. Figure 6a,b Illustrate the combined effect of the interaction between the solid-to-liquid ratio and temperature on Zn recovery using a three-dimensional surface plot and a contour diagram. Zn recovery increased with rising temperature at low solid-to-liquid ratio. However, at high solid-to-liquid ratio, Zn recovery decreased considerably. Figure 6c,d show that Zn recovery increased with increasing solid-to-liquid ratio and leaching time up to an optimum point, after which recovery values decreased. Figure 6e,f show that the highest Zn recovery was achieved within the range of 3–3.5 M acid concentration and 57–63 min leaching time. The optimal operating range was determined within the investigated parameter ranges.

Increasing temperature at low solid ratios supports Zn dissolution. However, at high solid ratios (9%–12% w/v), the effect of temperature is significantly reduced, as shown in Figure 6a,b. This behavior may be associated with reduced reagent accessibility to mineral surfaces and the increased influence of pulp density under high solid loading conditions [3,20]. The statistically significant temperature–acid concentration interaction (AD) indicates that temperature is most effective at moderate acid concentrations. At low acid concentrations, limited proton availability may restrict dissolution, whereas at high acid concentrations, the buffering effect associated with carbonate dissolution may reduce

the contribution of temperature to Zn recovery. In this case, temperature should not be considered as an independent variable, but rather together with the solid-to-liquid ratio and acid concentration. Similar observations have been reported in studies on the leaching of sulfide ores containing complex carbonates [3,26].

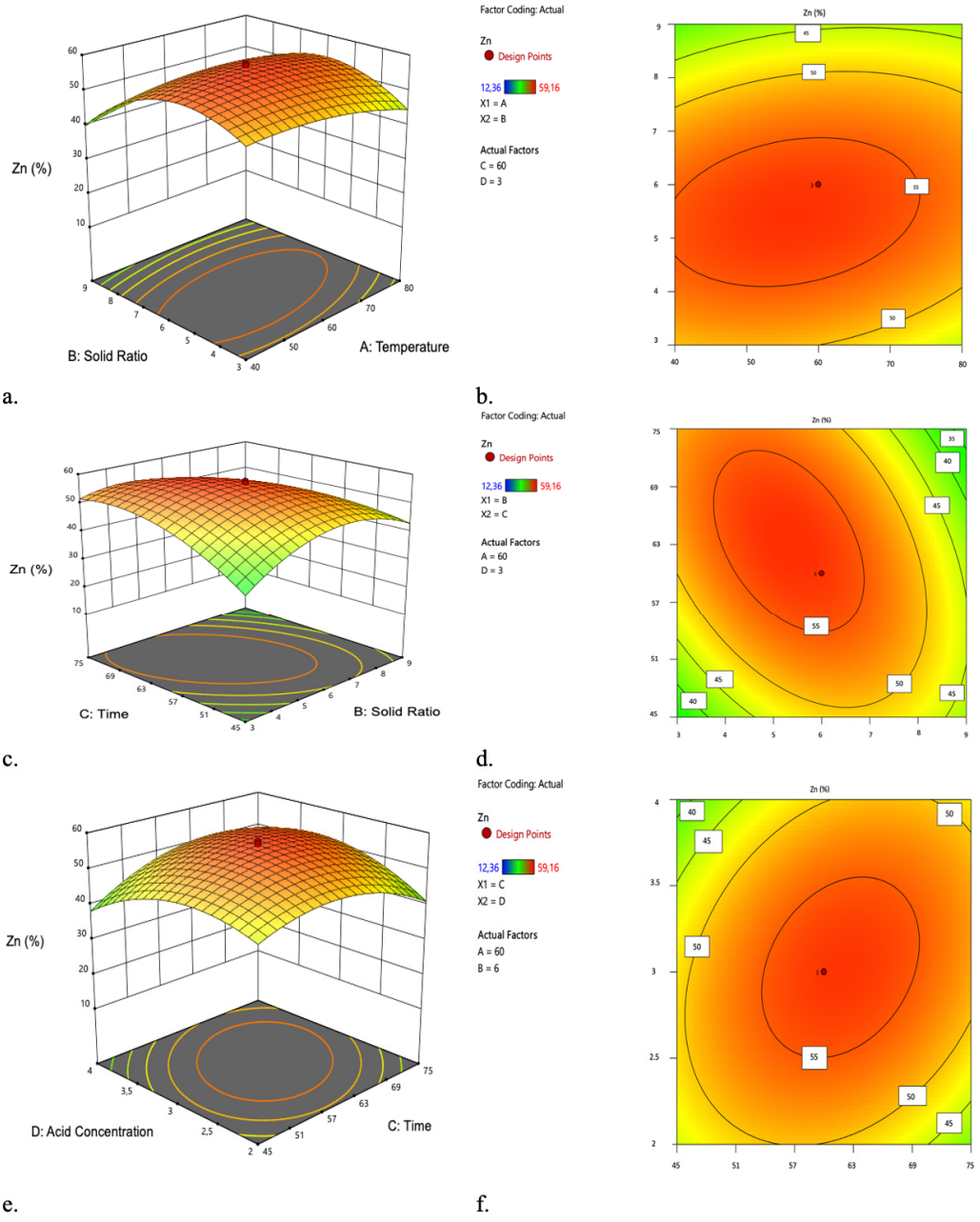


Figure 6. Three-dimensional graphs showing the interacting variables for Zn recovery: (**a**) Interaction between solid-to-liquid ratio and temperature. (**b**) Contour diagram of the effect of solid-to-liquid ratio and temperature on Zn recovery. (**c**) Interaction between leaching time and solid-to-liquid ratio. (**d**) Contour diagram of the effect of time and solid-to-liquid ratio on Zn recovery. (**e**) Interaction between acid concentration and time. (**f**) Contour diagram of the effect of acid concentration and time on Zn recovery.

Although chemical leaching was carried out under relatively strong operating conditions, the maximum Zn recovery remained limited to 59.16%. One of the main reasons for this behavior is the carbonate-rich nature of the ore, which resulted in significant acid consumption during leaching. Carbonate dissolution reduced the amount of free acid

available for sphalerite dissolution and therefore lowered the overall leaching efficiency. In addition, the formation of elemental sulfur on the mineral surface may have caused passivation, restricting further contact between the leaching solution and sphalerite particles. The possible formation of secondary precipitates under acidic conditions may also have contributed to surface coverage and reduced zinc dissolution. Furthermore, the negative effect of high solid/liquid ratios observed in the statistical analysis suggests that increased pulp density reduced the effectiveness of reagent–mineral interactions. The combined influence of these factors likely limited Zn recovery under the investigated conditions.

Figure 7a,b show that the parallel arrangement of the contour lines and the linear behavior of Fe recovery indicate a weak interaction between temperature and solid-to-liquid ratio. This suggests that the effects of these variables on Fe recovery are largely independent. Similarly, Figure 7c,d demonstrate that the interaction between leaching time and temperature is limited, indicating that these parameters affect Fe recovery independently.

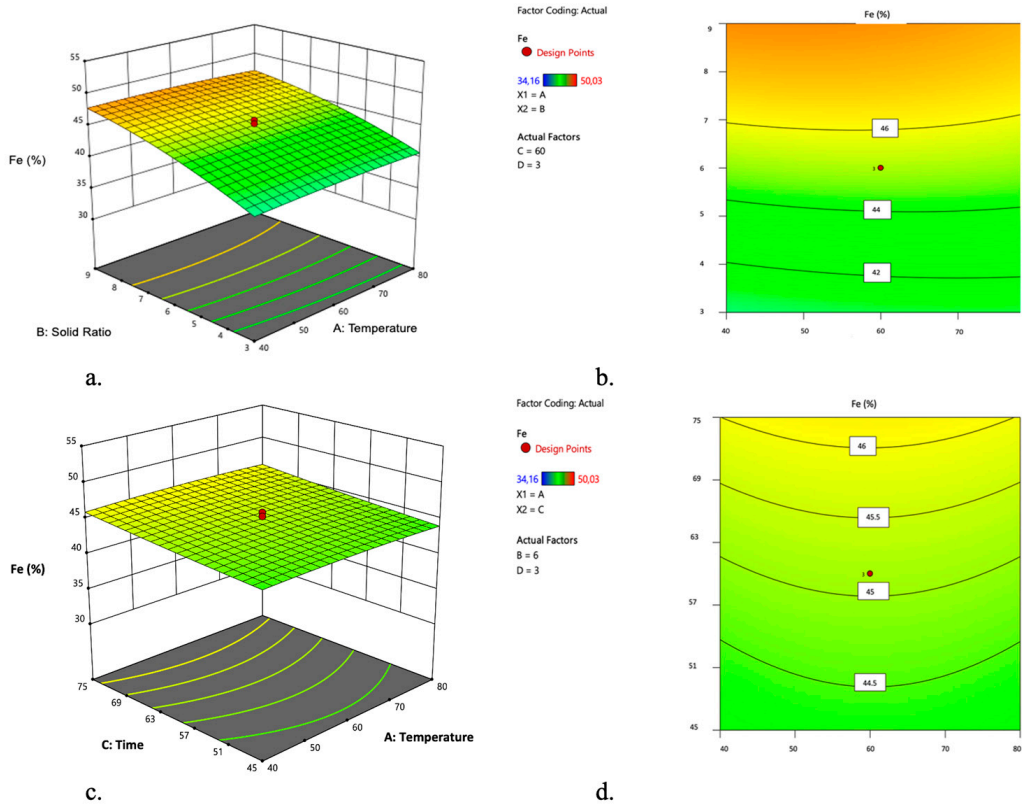


Figure 7. Three-dimensional graphs showing the interacting variables for Fe recovery: (**a**) Interaction between solid-to-liquid ratio and temperature. (**b**) Contour diagram of the effect of solid-to-liquid ratio and temperature on Fe recovery. (**c**) Interaction between leaching time and temperature. (**d**) Contour diagram of the effect of leaching time and temperature on Fe recovery.

3.4. Statistical Modeling and Model Validation for Bioreactor-Based Bioleaching

The bioleaching process of the sphalerite sample using *A. ferrooxidans* was evaluated based on a Central Composite Design (CCD). The effects of the independent variables, including solid-to-liquid ratio (%), pH, and Fe(II) concentration (g/L), were investigated. The RSM–CCD matrix consisted of 17 experimental runs, including factorial, axial, and center points, ensuring reliable estimation of linear, quadratic, and interaction effects. The corresponding Zn and Fe recoveries are presented in Table 6.

Table 6. Experimental design matrix and corresponding Zn and Fe recoveries for bioleaching.

Experiment No	pH (A)	S/L (% *w*/*v*) (B)	Fe (II) (g/L) (C)	Zn (%)	Fe (%)
1	1.4	7	2	17.87	53.14
2	1.6	5	4	22.34	30.47
3	1.8	3	2	25.54	14.03
4	1.6	5	8	19.92	22.54
5	1.4	3	6	32.09	20.89
6	1.4	3	2	33.12	26.41
7	1.8	7	6	9.27	31.13
8	1.8	7	2	10.44	38.74
9	1.6	1	4	37.26	3.89
10	1.6	5	4	19.23	19.71
11	1.2	5	4	28.44	33.98
12	1.6	9	4	9.47	48.45
13	1.8	3	6	21.57	10.21
14	1.6	5	4	24.41	17.31
15	1.4	7	6	17.23	47.86
16	2	5	4	16.6	13.11
17	1.6	5	0	19.01	34.17

Experimental results showed that Zn recovery ranged from 9.27% to 37.26%, while Fe recovery ranged from 3.89% to 53.14%. ANOVA was applied to assess the significance of the interactions among the operational parameters on the bioleaching performance. Zn and Fe recoveries were expressed using linear regression models. The regression models are presented in Equations (4) and (5). The independent variables used in the construction of the ANOVA equations were coded as pH (A), solid-to-liquid ratio (B), and Fe (II) concentration (C). The R^2 values were 0.9593 for Zn leaching and 0.9082 for Fe leaching. The predicted R^2 values were 0.9323 and adjusted R^2 = 0.9499 for Zn and predicted R^2 = 0.8680 and adjusted R^2 = 0.8871 for Fe. These values indicate a strong agreement between the experimental data and the model predictions. Furthermore, the close agreement between the adjusted R^2 and predicted R^2 values for Zn and Fe recoveries indicates that the developed models possess satisfactory predictive capability.

$$\text{Zn \%} = +21.18 - 3.57A - 7.53B - 0.3119C \quad (4)$$

$$\text{Fe \%} = +27.78 - 6A + 12.50B - 2.84C \quad (5)$$

In bioleaching experiments, Fe recovery is observed at high solid-to-liquid ratios and low pH values. However, Fe detected in the solution is also seen in the presence of gangue minerals such as pyrite, in addition to efficient mineral dissolution. In high pulp density and carbonate-rich environments, at pH ranges of 1.5–2.0, dissolved Fe^{3+} may precipitate jarosite ($KFe_3(SO_4)_2(OH)_6$). This consumes Fe^{3+} in the solution; thus, it reduces the availability of the oxidizing agent required for sphalerite dissolution and contributes to surface passivation [2,18]. Despite continuous pH control to maintain bacterial activity, jarosite precipitation may occur during carbonate dissolution at high solid-to-liquid ratios. This precipitation accelerates the consumption of Fe^{3+} used as an oxidizing agent. This further restricts Zn dissolution. Furthermore, the consumption of Fe^{3+} weakens the role of Fe (II) concentration as a process variable. This explains why Fe (II) concentration has a limited effect on bioleaching performance in the present study.

According to the ANOVA results for Zn and Fe recovery presented in Tables 7 and 8, the developed models and parameters were found to be statistically significant ($p < 0.05$). This indicates that the investigated variables had significant effects on metal recovery. According to the RSM analysis, the lack-of-fit F-values obtained for Zn (0.39) and Fe (0.37) were not significant compared with the pure error, indicating that the developed models adequately represented the experimental data without significant bias.

Table 7. Analysis of variance (ANOVA) results for Zn recovery obtained from the RSM-CCD model.

Source	Sum of Squares	df	Mean Square	F-Value	*p*-Value	
Model	1011.98	3	337.33	102.09	<0.0001	significant
A-PH	204.28	1	204.28	61.82	<0.0001	
B- S/L (% *w*/*v*)	806.14	1	806.14	243.97	<0.0001	
C-Fe (II) (g/L)	1.56	1	1.56	0.4710	0.5046	
Residual	42.96	13	3.30			
Lack of Fit	29.36	11	2.67	0.3926	0.8767	not significant
Pure Error	13.60	2	6.80			
Cor Total	1054.93	16				

Table 8. Analysis of variance (ANOVA) results for Fe recovery obtained from the RSM-CCD model.

Source	Sum of Squares	df	Mean Square	F-Value	*p*-Value	
Model	2928.53	3	976.18	42.89	<0.0001	significant
A-PH	575.16	1	575.16	25.27	0.0002	
B- S/L (% *w*/*v*)	2224.04	1	2224.04	97.71	<0.0001	
C-Fe (II) (g/L)	129.33	1	129.33	5.68	0.0331	
Residual	295.89	13	22.76			
Lack of Fit	197.65	11	17.97	0.3658	0.8913	not significant
Pure Error	98.24	2	49.12			
Cor Total	3224.42	16				

The adequacy of the RSM–CCD model was evaluated using diagnostic plots. The plot comparing the predicted and experimental Zn recovery values (Figure 8a) shows that the data points are closely distributed along the diagonal line, indicating strong agreement between the model predictions and the experimental results. The plot of standardized residuals versus experimental run order (Figure 8b) indicates that the error distribution is random and does not exhibit any systematic trend. The normal probability plot (Figure 8c) demonstrates that the residuals are normally distributed, while the plot of residuals versus predicted values (Figure 8d) indicates homogeneity of variance. These results confirm that the developed model adequately represents the experimental data and possesses satisfactory predictive capability.

Figure 9a,b present surface and contour plots illustrating the combined effect of pH and solid-to-liquid ratio on Zn recovery. The parallel and linear nature of the contour lines indicates that the interaction effect on Zn recovery is limited. Increasing the solid-to-liquid ratio likely reduced bacterial activity, thereby negatively affecting metal dissolution. Since changes in pH directly influence bacterial activity, they also affect bioleaching performance and Zn recovery.

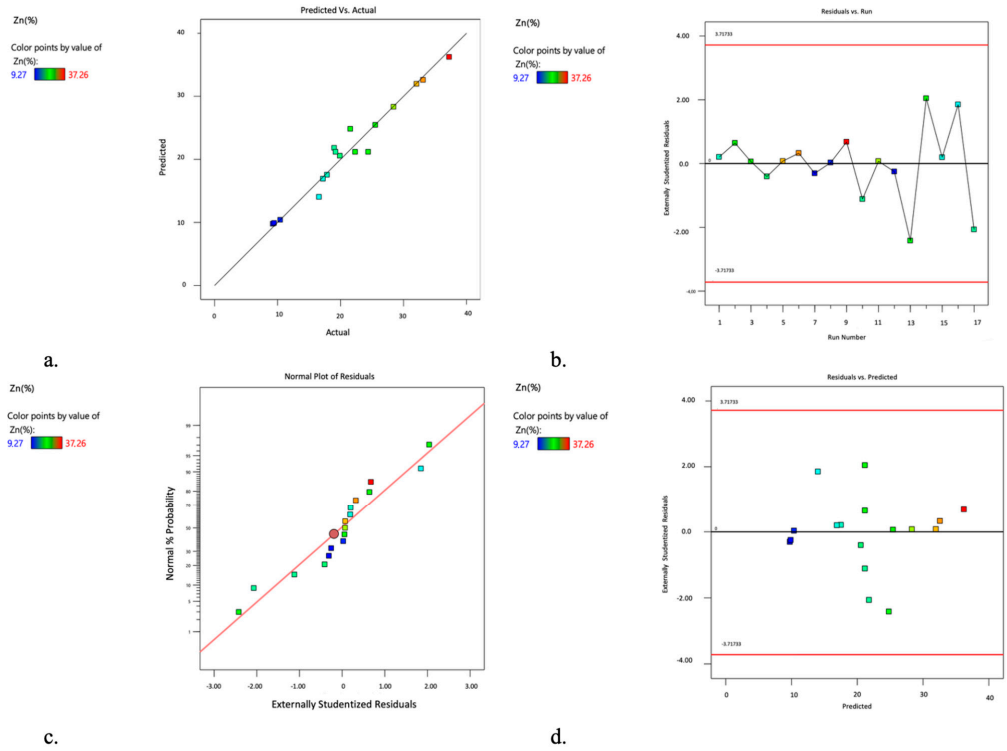


Figure 8. Diagnostic graphs for Zn recovery: (**a**) predicted responses vs. the actual values; (**b**) internal residuals vs. run number; (**c**) a plot of normal probability vs. the internal residuals; (**d**) internal residuals vs. the predicted response.

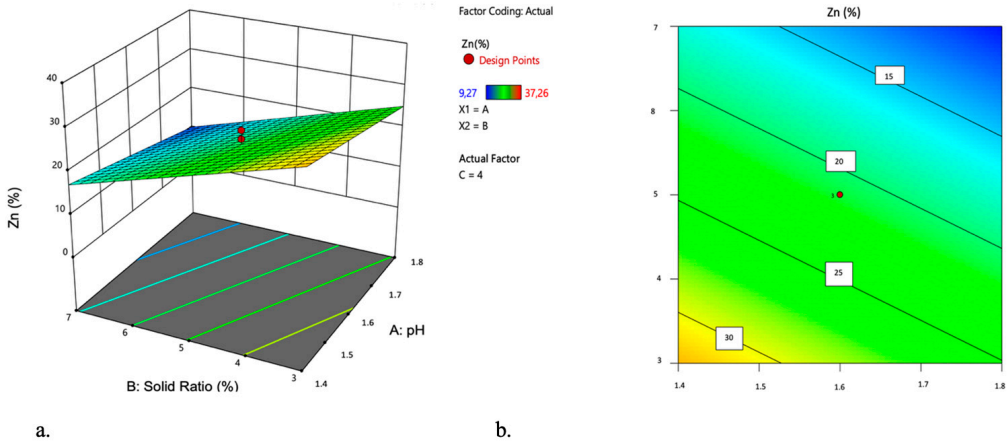
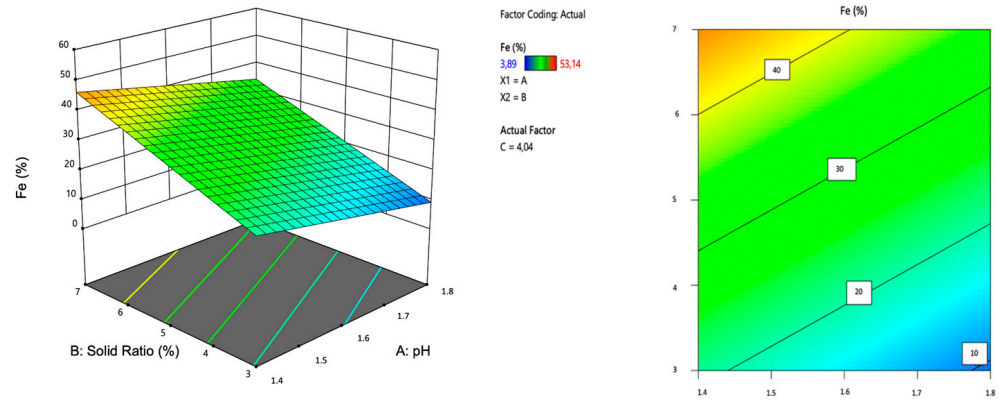


Figure 9. Three-dimensional graphs showing the interacting variables for Zn recovery: (**a**) Interaction between pH and solid-to-liquid ratio. (**b**) Contour diagram of the effect of pH and solid-to-liquid ratio on Zn recovery.

Figure 10a,b show the effects of pH and solid-to-liquid ratio on Fe recovery. The parallel and linear nature of the contour lines indicates that the interaction between the variables is weak and that the response can be adequately described by a linear model. The investigated parameters showed significant effects on Fe recovery. According to the experimental findings, the limited effect of Fe(II) concentration on the leaching system was mainly may associated with physicochemical constraints rather than iron availability. In bioreactor-based bioleaching, the oxidation of Fe^{2+} to Fe^{3+} plays an important role in sulfide mineral dissolution. Although the pH was periodically adjusted using sulfuric acid during the experiments, the carbonate-rich structure of the ore continuously increased the system pH due to high acid consumption. In addition, at high solid-to-liquid ratios, the

formation of elemental sulfur and iron precipitates on the ore surface may reduce leaching efficiency by creating passivation layers.



a. b.

Figure 10. Three-dimensional graphs showing the interacting variables for Fe recovery: (**a**) Interaction between pH and solid-to-liquid ratio. (**b**) Contour diagram of the effect of pH and solid-to-liquid ratio on Fe recovery.

3.5. Bacterial Activity During Bioleaching

To monitor bacterial activity during biological leaching experiments, cell counts were performed on day 0, 3, 6, 12, 15, 18 and 20 (Figure 11). As shown in Figure 11, cell counts indicate the period when *A. ferrooxidans* adapted to the ore pulp medium between days 0 and 3. From day 6 onwards, cell counts showed a continuous increase. Maximum values of 1.8–2.0 $\times$ 10^8 cells/mL were reached around day 15. This increase indicates active bacterial growth and sustained Fe^{2+} oxidation activity. Towards the end of days 15–20, cell counts decreased and stabilized. These observations confirm that *A. ferrooxidans* remained metabolically active throughout the 20-day biological leaching process under all experimental conditions.

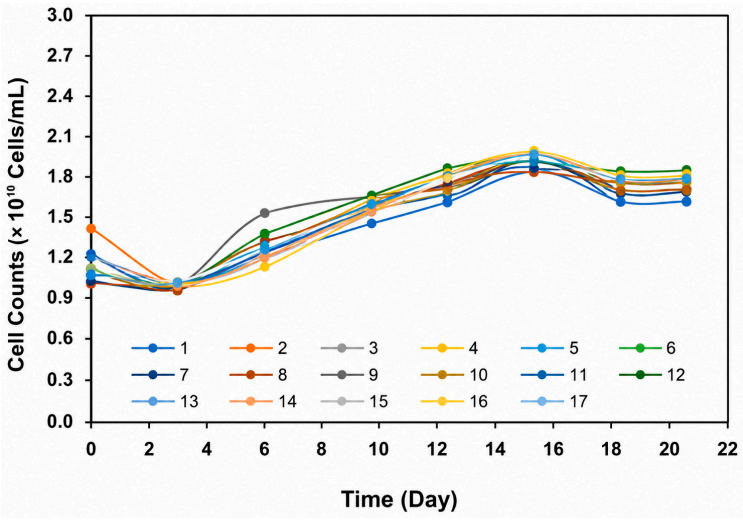


Figure 11. Cell counts of *A. ferrooxidans* during 20-day bioleaching experiments.

4. Discussion

Comparative Evaluation of Chemical and Biological Leaching

The investigation of chemical and biological leaching methods for zinc recovery from carbonate-rich sphalerite ore, based on process parameters, was carried out using central compound design approaches in the surface response method. Previous studies have mostly

dealt with these two methods separately and their examination from a statistical design perspective has been limited; therefore, this study fills a significant gap in the literature.

Although the operating parameters examined in chemical leaching and bioleaching studies on the same sphalerite ore differ, both processes were evaluated using the same response variables (Zn and Fe recovery). Therefore, this study focuses on the overall process performance, dominant control mechanisms, and operating characteristics. Since both processes inherently require different operating conditions and independent variables, the results obtained are interpreted as a process-level evaluation, not a direct comparison.

While zinc recovery in chemical leaching experiments was achieved at an efficiency of approximately 59.16%, the maximum recovery rate in bioleaching experiments using *A. ferrooxidans* was limited to 37.26% (Figure 12). This indicates that, in the short term, sulfuric acid leaching is more effective and efficient compared to bioleaching.

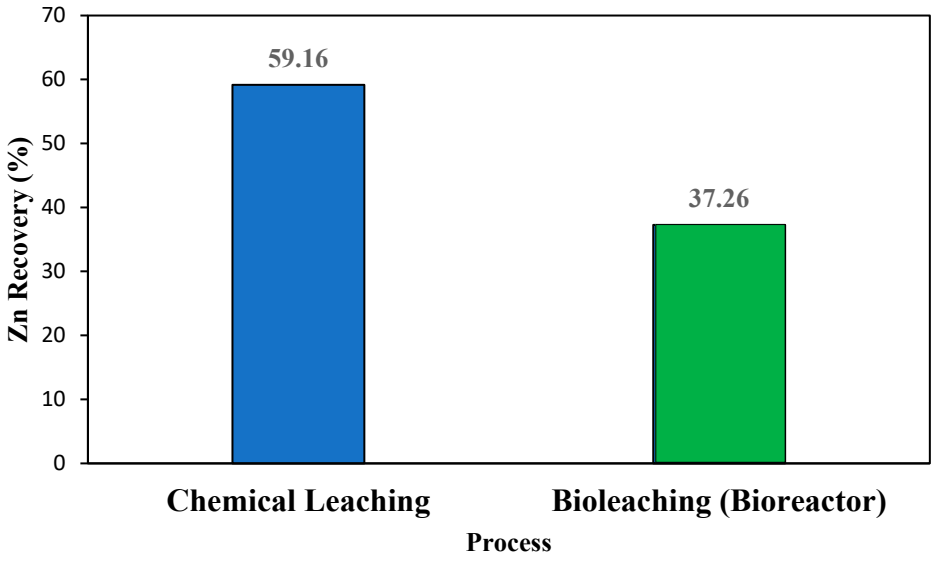


Figure 12. Comparative maximum Zn recovery obtained by chemical leaching and bioreactor-based bioleaching processes.

In chemical leaching experiments, leaching time and its interactions with other variables were the primary drivers of dissolution efficiency, while temperature and acid concentration showed limited individual effects under the investigated conditions [26,27]. In addition, the significance of solid-to-liquid ratio and leaching time in the ANOVA results indicates that these parameters strongly influenced the leaching efficiency. At high solid/liquid ratios, the leaching efficiency of Zn recovery was significantly reduced. In a previous study [28], lower dissolution efficiencies were observed at high pulp densities. In addition, in carbonate-rich ore bioleaching experiments, sulfuric acid was periodically added to maintain a suitable pH range for the growth and of *A. ferrooxidans*. The continuous consumption of protons during the dissolution of carbonate minerals may have led to a decrease in the acidity required for sphalerite dissolution and contributed to the lower Zn recovery observed in the bioleaching process. Although the total sulfuric acid consumption was not quantitatively determined, the observed pH behavior and the need for repeated acid additions indicate that carbonate minerals have a significant buffering effect. Furthermore, although acid concentration was not significant as an individual factor, its significance in interaction terms demonstrates the nonlinear behavior of the leaching system [27]. These findings suggest that simply increasing acid concentration may not always improve dissolution efficiency in complex carbonate-rich ores.

In the bioreactor-based leaching experiment, dissolution occurs through the oxidation of Fe^{2+} to Fe^{3+} by *A. ferrooxidans* [29,30]. However, elemental sulfur accumulation on the

mineral surface during the reaction can reduce the leaching rate by forming a passivation layer. Similar observations were also made in [3], and it was noted that sulfur accumulation is one of the main factors limiting the progress of dissolution. For this reason, the recovery achieved over the 20-day period remained limited. In bioleaching, pH and solid-to-liquid ratio are the most important parameters. The acidic pH range increases bacterial activity [28,29]; this is consistent with the optimum pH (1.2–2.0) used for *A. ferrooxidans* bacteria in previous studies. High solid-to-liquid ratio negatively affected dissolution efficiency. This situation was shown by Haghshenas et al. [10], who demonstrated that high pulp density reduces the Zn dissolution rate in sphalerite bioleaching of *A. ferrooxidans.* Additionally, the relationship between oxygen transfer and microbial activity directly influences bioleaching performance [31]; this indicates that the air-fed bioreactor system used in the present study aimed to maintain dissolved oxygen supply and bacterial activity.

The high carbonate content (calcite) of the ore is one of the key factors limiting bioleaching performance. The carbonate-rich structure caused acid consumption and increases in pH during the bioleaching process, which may have negatively affected bacterial activity and bioleaching efficiency [5]. Additionally, conducting the bioleaching process in a controlled bioreactor provides significant advantages in terms of process control and scalability compared to many studies in the literature. The air-fed bioreactor system ensured homogeneous mixing, enhanced dissolved oxygen supply, and maintained the sustainability of bacterial activity throughout the process.

In bioleaching experiments, the individual effect of pH on Zn recovery in the RSM design was found to be statistically limited. The carbonate-rich sample buffered pH levels towards higher values. However, since bacterial activity continued in the pH 1.2–2.0 range, acid was added periodically. Therefore, the pH value did not change to a level that would create statistically significant differences.

The most significant difference between the two processes is the reaction time. In chemical leaching, the optimum zinc recovery (59.16%) was achieved within 75 min, whereas the maximum bioleaching recovery (37.26%) required 20 days. This difference is mainly attributed to the relatively slow oxidation kinetics of *A. ferrooxidans* which relies on the Fe^{2+}/Fe^{3+} redox cycle for mineral dissolution. From an industrial perspective, the considerably shorter processing time of chemical leaching provides a significant advantage in terms of throughput and production capacity.

Furthermore, it appears that acid is used significantly in the two processes. In chemical leaching, sulfuric acid directly acts as the leaching reagent and its consumption is strongly influenced by the carbonate-rich nature of the ore. During bioleaching, periodic sulfuric acid additions were also required to maintain suitable pH conditions for bacterial activity due to carbonate dissolution and buffering effects. Although the cumulative acid consumption during bioleaching was not quantified, the necessity for repeated pH adjustments indicates that carbonate minerals significantly increased acid demand in both processes.

In terms of operating conditions, chemical leaching requires elevated temperatures (20–100 °C), whereas bioleaching is conducted at 30 ± 2 °C, which corresponds to the optimum growth temperature of *A. ferrooxidans*. Consequently, bioleaching generally requires lower energy input for heating and may offer reduced operating costs associated with temperature control.

Chemical leaching is also less complex than bioleaching in terms of process operation. Chemical leaching mainly requires acid-resistant reactors, reagent storage systems, and conventional hydrometallurgical equipment. In contrast, bioleaching involves additional requirements such as bacterial culture preparation and maintenance, aeration systems, continuous pH monitoring and adjustment, sterile operating conditions, and biological process control. These factors increase process complexity and demand specialized operational

expertise. Although chemical leaching is more readily scalable for industrial applications, bioleaching may encounter additional challenges, particularly when treating carbonate-rich ores due to acid consumption and pH control requirements.

From an environmental perspective, bioleaching is generally considered more sustainable than chemical leaching. Chemical leaching often requires higher acid concentrations and elevated temperatures, which can increase reagent consumption and generate larger volumes of acidic waste. In contrast, bioleaching relies on naturally occurring microorganisms and typically operates under milder conditions, resulting in a lower environmental footprint. Furthermore, the use of closed bioreactor systems can minimize emissions and reduce environmental risks.

In general, chemical leaching appears to be more suitable for industrial applications due to its high efficiency. In contrast, bioreactor-supported bioleaching offers low energy requirements and environmental benefits. However, its performance is found to be limited in complex ores rich in carbonates. This study identifies the mechanisms determining process selection in complex sphalerite systems and demonstrates the need to evaluate bioleaching within hybrid systems. From an environmental perspective, chemical leaching poses risks due to high acid concentrations and temperatures. In contrast, bioleaching conducted in a bioreactor enhances process controllability, facilitates scalability at an industrial scale, and offers an environmentally friendly approach by limiting the use of hazardous chemicals.

5. Conclusions

This study systematically investigated zinc recovery from a carbonate-rich complex sphalerite ore using chemical leaching and bioreactor-based bioleaching combined with Response Surface Methodology (RSM). In sulfuric acid leaching, the maximum Zn recovery of 59.16% was achieved at a solid-to-liquid ratio of 3%, acid concentration of 4 M, temperature of 40 °C, and leaching time of 75 min. In the bioreactor-based bioleaching experiments conducted using *A. ferrooxidans*, the maximum Zn recovery reached 37.26% after 20 days under conditions of 1% solid-to-liquid ratio, pH 1.6, 4 g/L Fe (II), and 30 °C.

Statistical evaluation of the RSM–CCD results demonstrated that the solid-to-liquid ratio was one of the most influential parameters in both systems. In chemical leaching, increasing pulp density negatively affected Zn recovery due to reduced effective surface area, whereas leaching time positively influenced dissolution efficiency. The relatively limited effects of acid concentration and temperature suggest that the dissolution behavior was predominantly controlled by pulp density under the investigated conditions. In bioleaching, pH and solid-to-liquid ratio significantly affected Zn recovery, indicating the strong dependence of microbial activity on physicochemical conditions. Furthermore, the carbonate-rich structure of the ore increased acid consumption and contributed to pH instability during bioleaching.

Overall, the results demonstrated that chemical leaching provided higher Zn recovery than bioleaching under the investigated conditions. The developed statistical models successfully described the leaching behavior and provided useful information for the optimization of zinc recovery from complex carbonate-rich sphalerite ores. In chemical leaching and bioleaching experiments, process operating parameters consist of different independent variables. The comparison presented in this study should not be interpreted as a direct comparison carried out under the same experimental conditions, but rather as a comparative evaluation of process performance, dominant control mechanisms, and operating characteristics.

Author Contributions: Project administration, Funding acquisition, Conceptualization, Data curation, Formal analysis, Writing—review and editing, E.K.; Conceptualization, Methodology, Investigation, Validation, Visualization, Writing—original draft, Writing—review and editing, Supervision, Z.Ç.; Writing—original draft, Writing—review and editing, Supervision, S.D.; Writing—review and editing, Supervision, D.Ç. All authors have read and agreed to the published version of the manuscript.

Funding: This work was supported by Scientific Research Projects Coordination Department of Atatürk University [Project No: FBA-2025-14869].

Data Availability Statement: The original contributions presented in this study are included in the article. Further inquiries can be directed to the corresponding author.

Conflicts of Interest: The authors declare no conflicts of interest.

References

1. Liao, M.; Deng, T. Zinc and lead extraction from complex raw sulfides by sequential bioleaching and acidic brine leach. *Miner. Eng.* **2004**, *17*, 17–22. [CrossRef]
2. Santos, S.M.C.; Machado, R.M.; Correia, M.J.N.; Reis, M.T.A.; Ismael, M.R.C.; Carvalho, J.M.R. Ferric sulphate/chloride leaching of zinc and minor elements from a sphalerite concentrate. *Miner. Eng.* **2010**, *23*, 606–615. [CrossRef]
3. Sokić, M.; Bugarčić, M.; Jovanović, A. Sphalerite leaching in acid media: A review. *Metall. Mater. Data* **2023**, *1*, 33–43. [CrossRef]
4. Salvioli-Mariani, E.; Boschetti, T.; Vescovi, F.; Scacchetti, M.; Toscani, L.; Mattioli, M. Hydrothermal lead-zinc-copper mineralizations in sedimentary rocks of Northern Apennines (Italy). *J. Geochem. Explor.* **2024**, *257*, 107365. [CrossRef]
5. Olubambi, P.A.; Ndlovu, S.; Potgieter, J.H.; Borode, J.O. Effects of ore mineralogy on microbial leaching of low grade complex sulphide ores. *Hydrometallurgy* **2007**, *86*, 96–104. [CrossRef]
6. Bidari, E.; Windarni, C.W.; Godinho, J.R.A.; Frisch, G. Role of Oxidants in Metal Extraction from Sulfide Minerals in a Deep Eutectic Solvent. *ACS Omega* **2024**, *9*, 14592–14603. [CrossRef] [PubMed]
7. Murugappan, R.M.; Karthikeyan, M. Microbe-Assisted Management and Recovery of Heavy Metals from Electronic Wastes. In *Environmental Management of Waste Electrical and Electronic Equipment*; Elsevier: Amsterdam, The Netherlands, 2021; pp. 65–88. [CrossRef]
8. Anderson, C.G.; Harrison, K.D.; Krys, L.E. Process Integration of Sodium Nitrite Oxidation and Fine Grinding in Refractory Precious Metal Concentrate Pressure Leaching. In *Proceedings of the 17th International Precious Metals Conference, Warrendale, PA, USA, 1993*; AIME: Warrendale, PA, USA, 1993; pp. 19–44.
9. Mousavi, S.M.; Yaghmaei, S.; Vossoughi, M.; Jafari, A.; Roostaazad, R.; Turunen, I. Bacterial leaching of low-grade ZnS concentrate using indigenous strains. *Hydrometallurgy* **2007**, *85*, 59–65. [CrossRef]
10. Haghshenas, D.F.; Bonakdarpour, B.; Alamdari, E.K.; Nasernejad, B. Optimization of bioleaching parameters of sphalerite by *Acidithiobacillus ferrooxidans*. *Hydrometallurgy* **2012**, *111*, 22–28.
11. Ghosh, S.; Paul, A.K. Heterotrophic leaching of metals from Indian chromite mining overburden. *Int. J. Miner. Reclam. Environ.* **2017**, *31*, 66–77. [CrossRef]
12. Dutrizac, J.E. Dissolution of sphalerite in ferric sulfate media. *Metall. Mater. Trans. B* **2006**, *37*, 161–171. [CrossRef]
13. Aydogan, S.; Aras, A.; Canbazoglu, M. Dissolution kinetics of sphalerite in acidic ferric chloride leaching. *Chem. Eng. J.* **2005**, *114*, 67–72. [CrossRef]
14. Li, C.; Wei, C.; Xu, H.S.; Li, M.; Li, X.; Deng, Z.; Fan, G. Pressure leaching of sphalerite concentrate in sulfuric acid medium. *Hydrometallurgy* **2010**, *102*, 91–94.
15. Gupta, A.; Mishra, R. Recovery of zinc from Moore cake. *Miner. Eng.* **2003**, *16*, 41–43. [CrossRef]
16. Pani, C.K.; Swain, S.; Kar, R.N.; Chaudhury, G.R.; Sukla, L.B.; Misra, V.N. Bio-dissolution of zinc sulfide concentrate in continuous bioreactor. *Miner. Eng.* **2003**, *16*, 1019–1021.
17. Deveci, H.; Akcil, A.; Alp, I. Bioleaching of complex zinc sulphides. *Hydrometallurgy* **2004**, *73*, 293–303. [CrossRef]
18. Pina, P.D.S.; Leão, V.A.; Silva, C.A.D.; Daman, D.; Frenay, J. Effect of iron on sphalerite bioleaching. *Miner. Eng.* **2005**, *18*, 549–551. [CrossRef]
19. Abdollahi, H.; Mirmohammadi, M.; Ghassa, S.; Jozanikohan, G.; Boroumand, Z.; Tuovinen, O.H. Acid bioleaching of sphalerite samples. *Hydrometallurgy* **2022**, *212*, 105897. [CrossRef]
20. Picazo-Rodríguez, N.G.; Soria-Aguilar, M.J.; Martínez-Luévanos, A.; Almaguer-Guzmán, I.; Chaidez-Félix, J.; Carrillo-Pedroza, F.R. Direct acid leaching of sphalerite. *Minerals* **2020**, *10*, 359. [CrossRef]
21. Silva, G. Diffusion and reaction control in sphalerite leaching. *Hydrometallurgy* **2004**, *73*, 313–324. [CrossRef]
22. Petersen, J. From understanding the rate limitations of bioleaching mechanisms to improved bioleach process design. *Hydrometallurgy* **2023**, *221*, 106148. [CrossRef]

23. Lundstedt, T.; Seifert, E.; Abramo, L.; Thelin, B.; Nyström, Å.; Pettersen, J.; Bergman, R. Experimental design and optimization. *Chemom. Intell. Lab. Syst.* **1998**, *42*, 3–40. [CrossRef]
24. Bezerra, M.A.; Santelli, R.E.; Oliveira, E.P.; Villar, L.S.; Escaleira, L.A. Response surface methodology. *Talanta* **2008**, *76*, 965–977. [CrossRef] [PubMed]
25. Alanazi, K.; Georgiou, S.; Koukouvinos, C.; Stylianou, S. Central composite designs with three missing observation. *Appl. Numer. Math.* **2025**, *208*, 2–21.
26. Nnanwube, I.; Onukwuli, O.; Ezekannagha, C. Kinetics of sphalerite dissolution. *Can. Metall. Q.* **2024**, *63*, 1592–1603. [CrossRef]
27. Shahrezaei, F.; Karimi, S.; Behnajady, B. Experimental and dynamic molecular study of zinc extraction from sphalerite concentrate in ternary deep eutectic solvent. *Colloids Surf. A* **2024**, *695*, 134241. [CrossRef]
28. Nozari, I.; Azizi, A. Copper dissolution kinetic modeling. *J. Sustain. Metall.* **2020**, *6*, 437–450. [CrossRef]
29. Pedersen, T.F. Tailings disposal considerations. In *Waters in Peril*; Springer: Boston, MA, USA, 2001; pp. 151–162.
30. Tonietti, L.; Esposito, M.; Cascone, M.; Barosa, B.; Fiscale, S.; Muscari Tomajoli, M.T.; Sbaffi, T.; Santomartino, R.; Covone, G.; Cordone, A.; et al. Unveiling the bioleaching versatility of *Acidithiobacillus ferrooxidans*. *Microorganisms* **2024**, *12*, 2407. [CrossRef] [PubMed]
31. Kaksonen, A.H.; Boxall, N.J.; Gumulya, Y.; Khaleque, H.N.; Morris, C.; Bohu, T.; Cheng, K.Y.; Usher, K.M.; Lakaniemi, A.M. Recent progress in biohydrometallurgy and microbial characterisation. *Hydrometallurgy* **2018**, *180*, 7–25. [CrossRef]

Disclaimer/Publisher's Note: The statements, opinions and data contained in all publications are solely those of the individual author(s) and contributor(s) and not of MDPI and/or the editor(s). MDPI and/or the editor(s) disclaim responsibility for any injury to people or property resulting from any ideas, methods, instructions or products referred to in the content.